Materials and Interfaces

Synthesis of non-toxic pyrazolidine based benzoxazine coated cotton fabric for oil-water separation

Manoj Manickam, Prabunathan Pichaimani, Hariharan Arumugam, and Alagar Muthukaruppan

Ind. Eng. Chem. Res., **Just Accepted Manuscript** • DOI: 10.1021/acs.iecr.9b03440 • Publication Date (Web): 04 Nov 2019

Synthesis of non-toxic pyrazolidine based benzoxazine coated cotton fabric for oil-water separation.

Manoj Manickam, Prabunathan Pichaimani, Hariharan Arumugam, Alagar Muthukaruppan*

Polymer Engineering Laboratory, PSG Institute of Technology and Applied Research, Neelambur, Coimbatore - 641 062.

*Corresponding author: mkalagar@yahoo.com

Abstract

In the present work, pyrazolidine bisphenol (PYBP) based superhydrophobic/superoleophilic benzoxazine (PBz) matrices, were synthesized and described in comparison with bisphenol-F benzoxazines. The preliminary *in vitro* toxicity assay reveals the non-toxic nature of PYBP. Data obtained from thermal and surface studies indicate that the prepared PYBP based PBzs have enhanced thermal stability than those of bisphenol-F benzoxazines. Further, the prepared PYBP based PBzs coated cotton fabric displayed superior water contact angle (WCA=154.7°) and sliding contact angle (θ = 9°). Observations from SEM images suggest that the inherent superhydrophobic nature was due to the formation of rough surfaces. Furthermore, the oil-water separation was successfully ascertained from the appropriate experimental conditions using PYBP coated fabric. The separation efficiency and flux are found to be greater than 90 % after 10 cycles. Thus, the PYBP based superhydrophobic/superoleophilic polybenzoxazines (PBzs) have been synthesized and characterized to assess their suitability for water repellent and for oil-water separation applications.

Keywords: Pyrazolidine bisphenol, non-toxicity, polybenzoxazine, water contact angle, char yield, oil-water separation.

1. INTRODUCTION

Polybenzoxazine (PBz), a newly developed high performance thermoset polymer possess valuable properties, such as high thermal stability, low water absorption, superior chemical and flame resistance, nearly zero shrinkage and no by-product release upon curing.[1,2] The formation of an extensive inter- and intramolecular hydrogen bonding within the structure of polybenzoxazine contributes to an enhancement of its physical and mechanical properties.[3] Molecular design flexibility with different functional groups in the PBz skeleton is the advantage of this polymer and can be accessed easily by phenol, amine and formaldehyde as precursors.[4] For example, bisphenol-A (BPA) is considered as an important precursor for the preparation of conventional PBz resin due to its easy availability, high purity and inexpensive nature.[5] Hence, the preparation of BPA based benzoxazine monomers exceed 4.5 million tons every year. However, the genotoxicity and endocrine disrupting activity of the BPA causes serious health issues[6,7] and consequently BPA based plastics in food and beverage packing application is under scrutiny.[8] Owing to this fact, BPA

is increasingly replaced by structurally similar chemicals, in particular bisphenol-S (BPS) and bisphenol-F (BPF).[9,10] According to European Chemical Agency (ECHA) ECHA, 1000 to 10,000 million metric tons of BPS are manufactured or imported annually into the European economic area. But, no production data for BPF are currently registered, suggesting that BPF is still a low use chemical.[11,12] Therefore BPF based PBzs emerge as a class of new polymer materials for various applications. However, BPF also exhibit certain degree of toxic behavior, hence the development of alternative non-toxic precursor materials are warranted.[13]

On the other hand, BPA based PBzs are being replaced with other heterocyclic PBzs. These superior class of polymers accounts for their excellent mechanical performance, outstanding heat and flame retardant behaviour and improved molecular design flexibility when compared to those of conventional novolac, resole type phenolics and epoxy resins.[14] Apart from these, the value addition of these systems are high char yield, high glass transition temperature and amenability for noncatalytic polymerization.[15-18] Earlier, our group has prepared heterocyclic imidazole core bisphenol based benzoxazine monomers and polyimides and explored their potential applications.[19-21] Thus, our continued interest have motivated us to introduce pyrazolidine bisphenol as precursor to prepare novel benzoxazine monomers.

Recently, PBz have been utilized as coating material for technical textile fabrics in order to enhance the commercial value. Among the technical textiles, cotton fabrics have received great attention and have been used in wide multifunctional applications such as anti-corrosion, anti-fogging/frosting, anti-bioadhesion, and water-oil separation.[22-24] In order to explore the technical applications, the post-functionalization of cotton fabrics with different chemical additives were carried out.[25,26] Functionalized cotton fabric coated with different materials are found to possess superhydrophobic behaviour with higher values of water contact angle (WCA) and can be used for water-oil separation.[27] Conventional polybenzoxazine and its hybrid materials have been recently employed over different filtration medium in order to separate oil-water mixture.[28-30] However, no significant focus have been paved towards design and development of non-toxic benzoxazine monomers with superior hydrophobic behaviour.

With this perspective, the present work focus the possible replacement of toxic BPA with newly prepared pyrazolidine bisphenol (PYBP) and less toxic BPF for the preparation of PBzs and to study their application as superhydrophobic materials coated on the cotton fabrics. In this respect, the amines with inherent hydrophobic behaviour such as

dodecylamine (dda), octadecylamine (oda) and 4-fluoroaniline (fa)[31] were selected to synthesize corresponding benzoxazines (Schemes 1 and 2 mentioned in materials and method section). Data obtained from different studies are discussed and reported.

2. MATERIALS AND METHODS

2.1. Chemicals

BPF was obtained from Anabond Limited, Chennai, India. 4-Hydroxy benzaldehyde, 4-hydroxy acetophenone were purchased from Sigma Aldrich. Paraformaldehyde, dioxane, hydrazine hydrate, *para*-toluenesulphonic acid (PTSA) and acetic acid were obtained from Qualigens, India. Dodecylamine (dda), octadecylamine (oda) and 4-fluoroaniline were obtained from SRL, India. Anhydrous sodium sulphate, ethanol and ethylacetate were obtained from Loba chemicals, India. Cotton fabric was procured from textile industry in Erode, Tamilnadu, India.

2.2. Synthesis of 1-(3,5-bis(4-hydroxyphenyl)-4,5-dihydro-1*H*-pyrazol-1-yl)ethanone or pyrazolidine-bisphenol (PYBP)

1-(3,5-bis(4-hydroxyphenyl)-4,5-dihydro-1*H*-pyrazol-1-yl)ethanone or pyrazolidine-bisphenol (PyBF) was prepared in accordance with the reported literature[32] (Scheme 1) with slight modification. To a solution of 4-hydroxybenzaldehyde (7.55 g, 0.05 mol) and 4-hydroxyacetophenone (16.5 g, 0.05 mol) in ethanol (50 mL) PTSA (1.72 g, 0.01 mol) was added and refluxed for 5 h with constant stirring (Scheme 1). After the formation of product monitored through TLC, ethanol was removed partially and the reaction mixture was added to crushed ice to obtain the chalcone intermediate as yellow precipitate (Yield = 82%).

In the next step (Scheme 1), the chalcone (10 g, 0.042 mol) was dissolved in acetic acid (30 mL) and hydrazine monohydrate (21 mL, 0.042 mol) was added and refluxed for 6 h. After the formation of product monitored through TLC, the reaction mixture was cooled and added to crushed ice to obtain PYBP as light brown precipitate. The precipitate was filtered, washed with water and dried. The product was recrystallised using methanol (Yield = 76%). After re-crystallization the product was studied for structural confirmation using FTIR (Figure S2), ^{1}H-NMR (Figure S3) and MASS spectral analysis (Figure S4). ^{1}H-NMR, (DMSO-d_6): δ 2.24 (s, 3H), 2.99-3.05 (m, 1H), 3.69-3.76 (m, 1H), 5.37-5.41 (m, 1H), 6.66-

6.97 (m, 8H), 9.33 (s, 1H (OH)), 9.95 (s, 1H (OH)), ppm. MS : m/z = 296 (base peak = 295 appeared in negative mode).

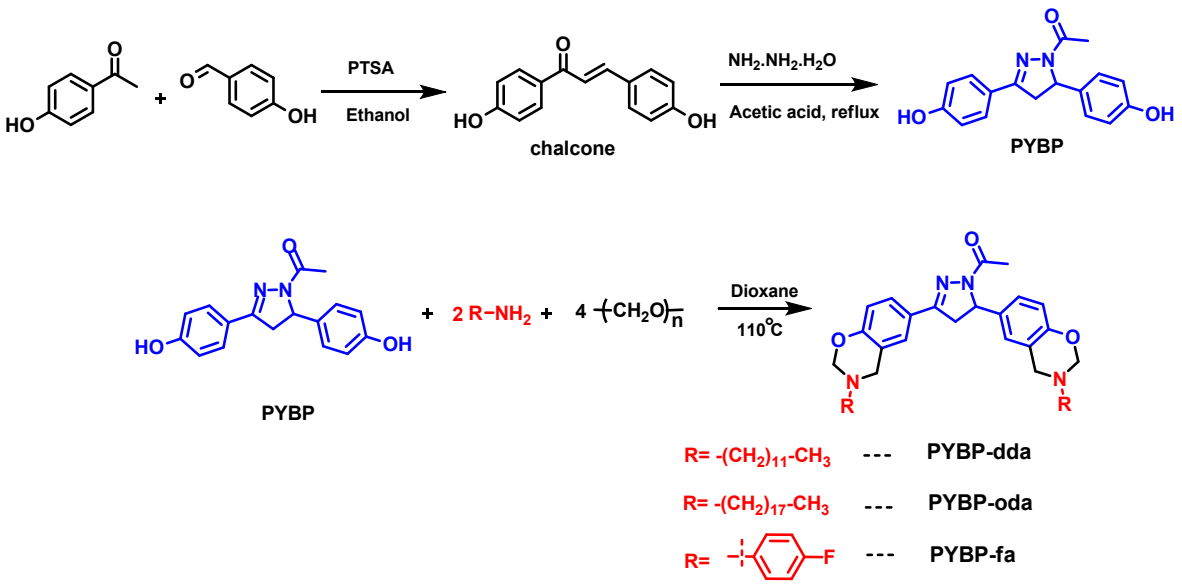

Scheme 1. Preparation of PYBF-dda, PYBF-oda and PYBF-fa

2.3. Preparation of pyrazolidine-bisphenol based benzoxazine monomer (PYBP-dda, PYBP-oda, PYBP-fa)

To prepare the benzoxazine monomer (Scheme 1), the bisphenol, PYBF (5 g, 0.17.90 mmol), respective amines (dodecylamine (dda), octadecylamine (oda) and 4-fluoroaniline (fa) 33.80 mmol) and paraformaldehyde (2.23 g, 74.35 mmol) were added separately to round bottomed flask containing 1,4-dioxane (8 mL) and slightly warmed to 60 °C to achieve homogeneity. Then the reaction temperature was raised to 110 °C and stirred for 15 h. The progress of the reaction was monitored by TLC. After the formation of the product, the reaction mixture was cooled, water was added and extracted using ethylacetate. To the organic layer, 10 M sodium hydroxide solution was added to remove any bisphenol residue present. The organic layer was dried over anhydrous sodium sulphate and evaporated under vacuum. The resultant products PYBP-dda, PYBP-oda and PYBP-fa were analysed for spectral studies.

2.4. Synthesis of bisphenol-F based benzoxazine monomer (BF-dda, BF-oda, BF-fa)

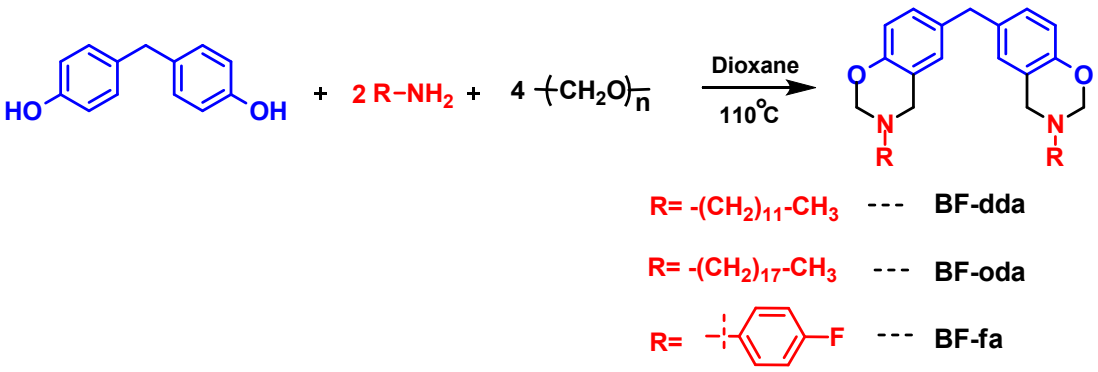

Scheme 2. Preparation of BF-dda, BF-oda and BF-fa

Bisphenol-F (10 g, 0.05 mol), respective amines (dodecylamine (dda)/octadecylamine (oda)/4-fluoroaniline (fa), 0.10 mol) and paraformaldehyde (6.6 g, 0.22 mol) were added separately to round bottomed flask containing 1,4-dioxane (10 mL) and slightly warmed to 60 °C to achieve homogeneity. Then the reaction temperature was raised to 110 °C and stirred for 12 h. The progress of the reaction was monitored by TLC. After the formation of the product, the reaction mixture was cooled, water was added and extracted using ethylacetate. To the organic layer, 10 M sodium hydroxide solution was added to remove any residual bisphenol present. The organic layer was dried over anhydrous sodium sulphate and evaporated under vacuum (Scheme 2). The prepared benzoxazine monomers were labelled in accordance with IUPAC nomelature as BF-dda, BF-oda and BF-fa and were preserved for further studies.

2.5. Assay for toxicity studies

The toxicity studies of BPA, BPF and the newly prepared pyrazolidine compound (PYBP) were checked in Human Embryonic Kidney (HEK) cells by MTT [3-(4,5-dimethylthiazol-2-yl)-2,5-diphenyltetrazolium bromide] assay.[33] HEK cells were grown (1×10^4 cells/well) in a 96-well plate for 48 h in to 75 % confluence. The medium was replaced with fresh medium containing serially diluted synthesized compounds (10, 25 and 50 µg/mL), and the cells were further incubated for 48 h. The culture medium was removed, and 100 µL of the MTT [3-(4,5-dimethylthiozol-2-yl)-3,5-diphenyl tetrazolium bromide] (Hi-Media) solution was added to each well and incubated at 37 °C for 4 h. After removal of the supernatant, 50 µL of dimethylsulfoxide was added to each of the wells and incubated for 10 min to solubilize the formazan crystals. The optical density (OD) was measured at 620 nm in

an ELISA multiwell plate reader (Thermo Multiskan EX, USA). The OD value was used to calculate the percentage of viability using the following formula.

$$\%\ of\ viability\ = \frac{OD\ value\ of\ experimental\ sample}{OD\ value\ of\ experimental\ control}\ X\ 100 \ldots\ldots\ldots\ldots\ldots\ldots (1)$$

2.6. Preparation of benzoxazines coated cotton fabrics

Nonwoven cotton fabrics were washed with distilled water and soaked in 2 M NaOH solution and heated to 100 °C for 3 h for the surface activation and removal of any greasy material.[34] After that the fabric was taken out and washed again with distilled water and kept drying at 60 °C for 10 h. After drying the pristine cotton fabrics were cut to appropriate sizes and weighed. Exactly 1 g of the BF and PYBP monomers were weighed separately in a beaker and 10 mL of THF was added and stirred for 10 minutes to completely dissolve the monomers. To the resulting BF and PYBP solutions the treated cotton fabrics were immersed in respective solutions and cured at 180 °C and 250 °C for 10 minutes individually. After curing the weight of the cotton fabrics were noted to ensure that all the coated fabrics have similar weight.

2.7. Characterisation

FTIR spectra measurements were carried out in Agilent Cary 630 FTIR Spectrometer. NMR spectra were recorded in Bruker (400 MHz) using deutrated chloroform ($CDCl_3$) and dimethylsulfoxide (DMSO-d_6) as a solvent and tetramethylsilane (TMS) as an internal standard. Mass spectra were recorded in Agilent mass spectrometer. DSC measurements were recorded using NETZSCH STA 449F3 under N_2 purge (60 mL min^{-1}) at scanning rate of 10°C min^{-1}. Thermogravimetric analysis (TGA) was obtained using NETZSCH STA 449F3 using 5 mg of sample under N_2 flow (60 mL min^{-1}) at heating rate of 20°C min^{-1}. The morphology of the matrices and composites are identified from an FEI QUANTA 200F high resolution scanning electron microscope (HRSEM). The water contact angle measurements of the coated fabric was conducted on a Dataphysicsinstrument (OCA 15, Germany) using a water drop (V = 10 μL) gently placed on the surface of the sample. The porosity of the fabrics were measured using capillary flow analysis from Porous Materials, Inc. Analytical Services, USA. The XPS was measured using an Omicron nanotechnology instrument at a pressure below 10^{-10} Torr. The tensile properties of the fabrics were measured using a

universal testing machine (Tensile Tester Z10 of Zwick/Roell, Germany), with a constant rate of extension. The test was done according to ASTM standard D5035-11 (Reapproved 2015).

3. RESULTS AND DISCUSSION

3.1. Toxicity studies

As mentioned earlier the toxicity of BPA restrict its application in various commerical products. There are few reports that state BPF also exhibit little toxicity.[13] In this regard, the newly prepared compound was analysed for *in vitro* toxicity against Human Embryonic Kidney (HEK) cells along with BPA and BPF. Figure S1 denote the morphology of cell under control (without compound) condition and at different concentrations against BPA, BPF and PYBP, respectively. In all the control, the cells were in normal structure. After treated with BPA, the morphology of the HEK cells were altered as observed in BPA (Figure S1). In case of BPF, morphology of the HEK cells were also slightly altered whereas the morphology of the HEK cells were not altered when they were treated with PYBP (Figure S1). The precise toxicity values in IC50 for the compounds BPA, BPF and PYBP were presented in Table S1 and Figure 1a-c.

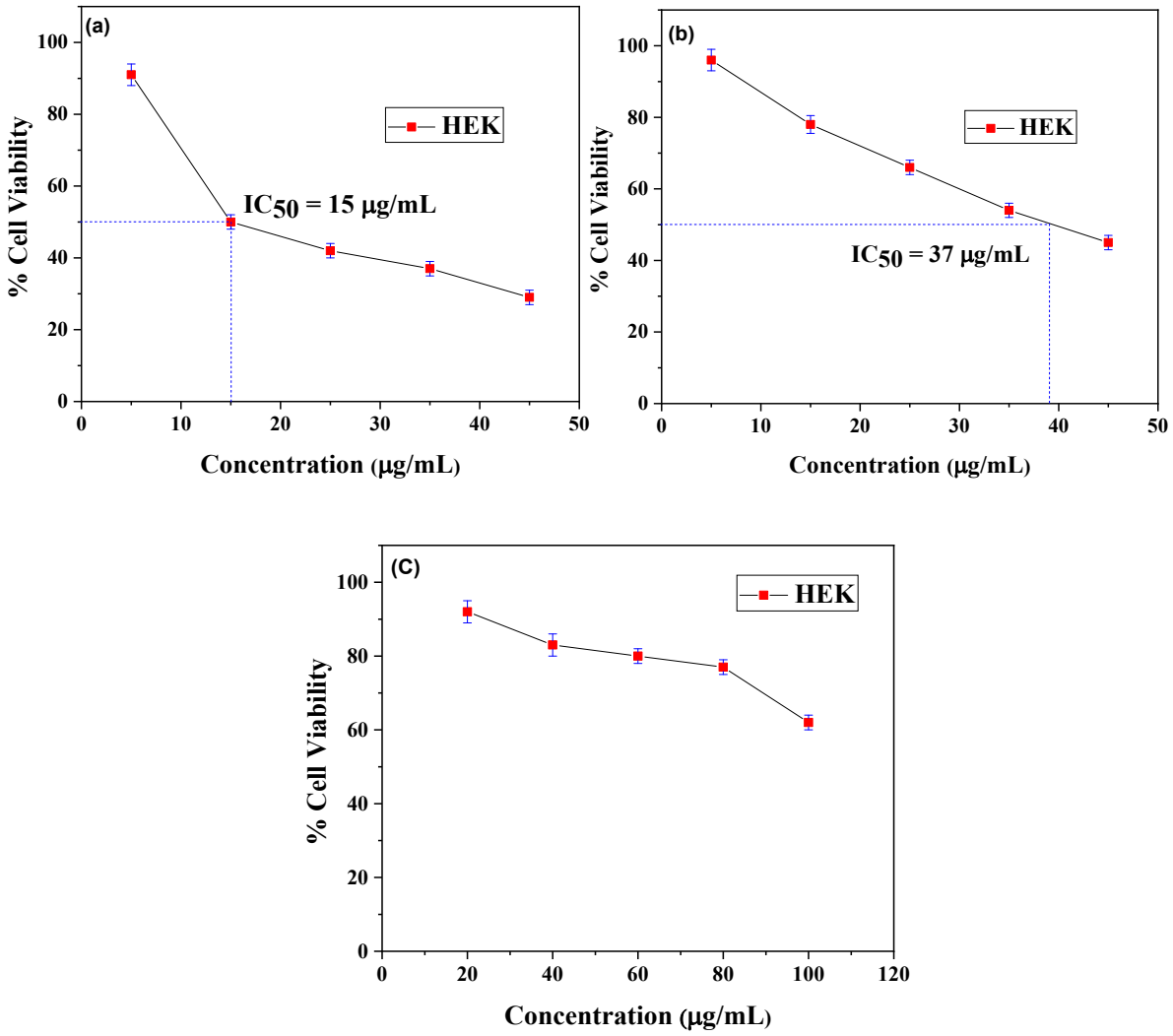

Figure 1. Human Embryonic Kidney cell viability (IC_{50}) against compouds (a) BPA, (b) BPF and (C) PYBP.

Table S1 presents the toxicity data of the compounds at 50 % inhibition concentration or half maximal inhibitory concentration. Among the compounds BPA shows IC_{50} = 15 µg/mL. which was same as the IC_{50} of cisplatin, IC_{50} = 15 µg/mL. Next BPF also exhibit a moderate toxicity exhibiting IC_{50} = 37 µg/mL. Interestingly the newly prepared compound PYBP do not exhibit any toxicity, IC_{50} > 100 µg/mL.

3.2. Chemical Structural Analysis of Benzoxazine Monomers

Figure 2 shows the FT-IR spectra of the benzoxazine monomers. The respective peaks appeared at 2915 cm^{-1} and 2853 cm^{-1} corresponds to the asymmetric and symmetric stretching vibrations of methylene group (-CH_2-) of oxazine ring as well as long alkyl side

chain of the dda and oda groups. The peaks appeared at 1242 cm^{-1} and 1090 cm^{-1} were attributed to the asymmetric and symmetric stretching vibrations of C-O-C bond of the benzoxazine monomer, respectively. The peak appeared at 1152 cm^{-1} represents the asymmetric stretching of C-N-C of benzoxazine monomer. Further, the appearance of peak at 1492 cm^{-1} corresponds to a tri-substituted benzene ring. Thus, based on the vibration peaks appeared, the formation of benzoxazine has been confirmed. [35,36] After thermal curing, the disappearance of peak at 916 cm^{-1}, confirms the ring opening polymerization of the monomer.

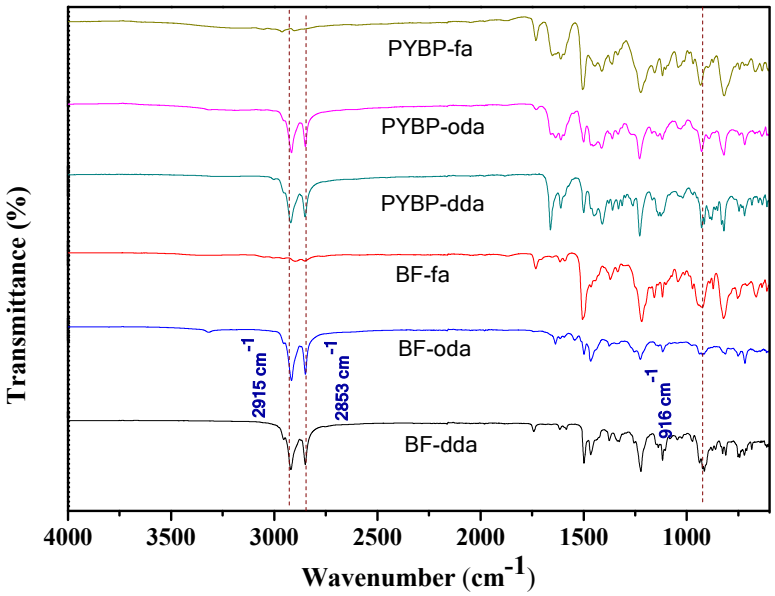

Figure 2. FTIR of Monomers BF and PYBP.

Further, the chemical structure of the monomers was confirmed by ^{1}H-NMR and ^{13}C-NMR. Figure 3 shows the ^{1}H-NMR spectra of BF-dda, BF-oda and BF-fa benzoxazine monomers. In the case of BF-dda, the formation of benzoxazine ring was confirmed by two singlets at δ 3.9 and δ 4.9 ppm in its ^{1}H-NMR spectrum. The methylene protons of BPF moiety appeared at δ 3.7 ppm. The aliphatic chain protons appeared at δ 1.0-2.0 ppm. The N-CH_2- protons showed a multiplet at δ 2.7 ppm. The ^{13}C-NMR spectrum of BF-dda (Figure S5) showed two signals at δ 67 and δ 82 ppm corresponding for the benzoxazine ring methylene carbons. The methylene carbon of the BPF moiety appeared at δ 60 ppm. The quarternary carbon of the benzoxazine ring adjacent to oxygen atom appeared in the deshielding region at δ 152 ppm.

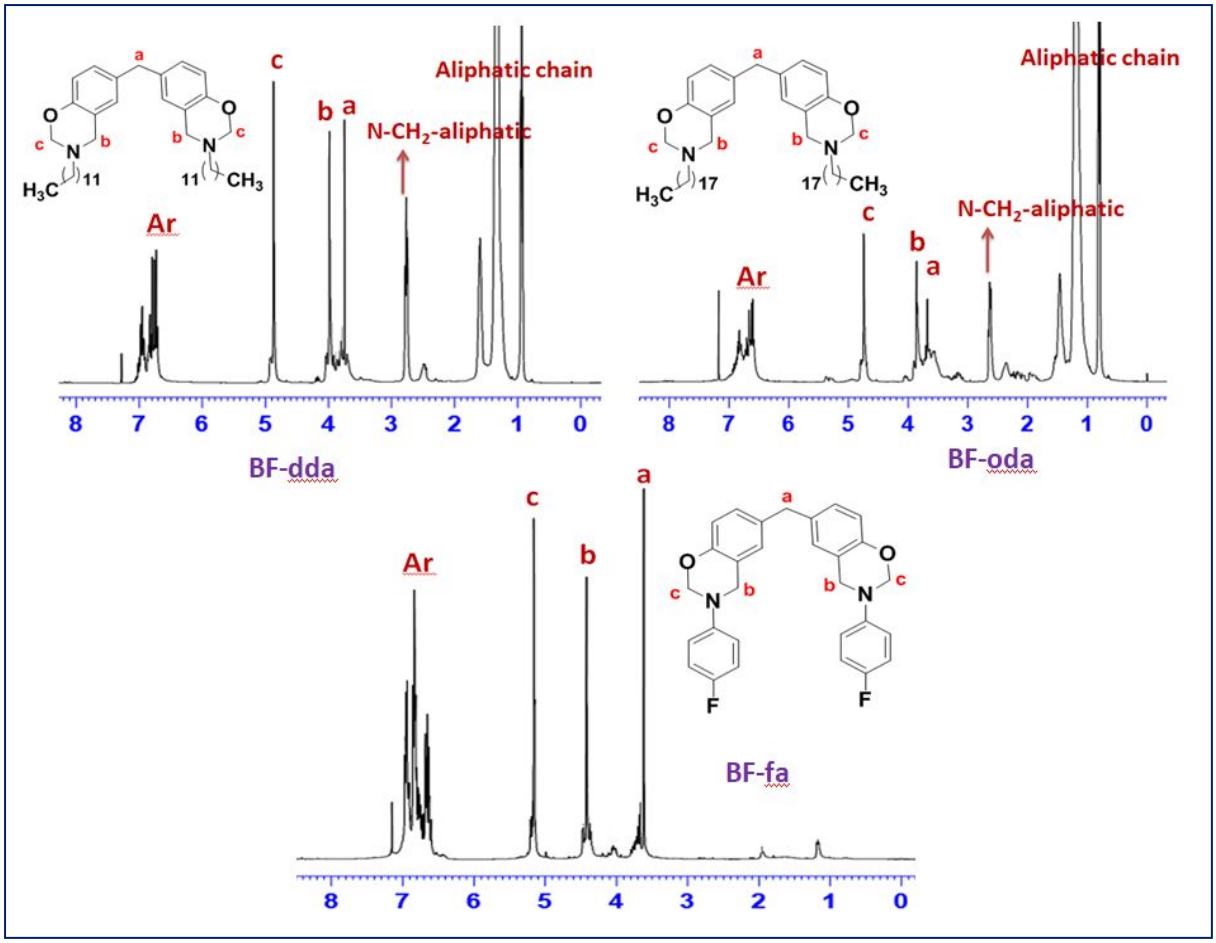

Figure 3. ^{1}H-NMR of monomers; BF-dda, BF-oda, BF-fa.

In case of BF-oda, the formation of benzoxazine ring was confirmed by two singlets at δ 3.9 and δ 4.8 ppm in its ^{1}H-NMR spectrum. The methylene protons of BF moiety appeared at δ 3.7 ppm. The aliphatic chain protons appeared at δ 0.8-2.0 ppm. The *N*-CH_2-protons showed a multiplet at δ 2.6 ppm. Aromatic protons appeared between δ 6.5 and 7.0 ppm. The ^{13}C-NMR spectrum of BF-oda (Figure S6) showed two signals at δ 66 and δ 80 ppm corresponding for the benzoxazine ring methylene carbons. The methylene carbon of the BF moiety appeared at δ 60 ppm. The quaternary carbon of the benzoxazine ring adjacent to oxygen atom appeared in the deshielding region at δ 152 ppm. Mass spectrum of BF-oda is shown in Figure S7.

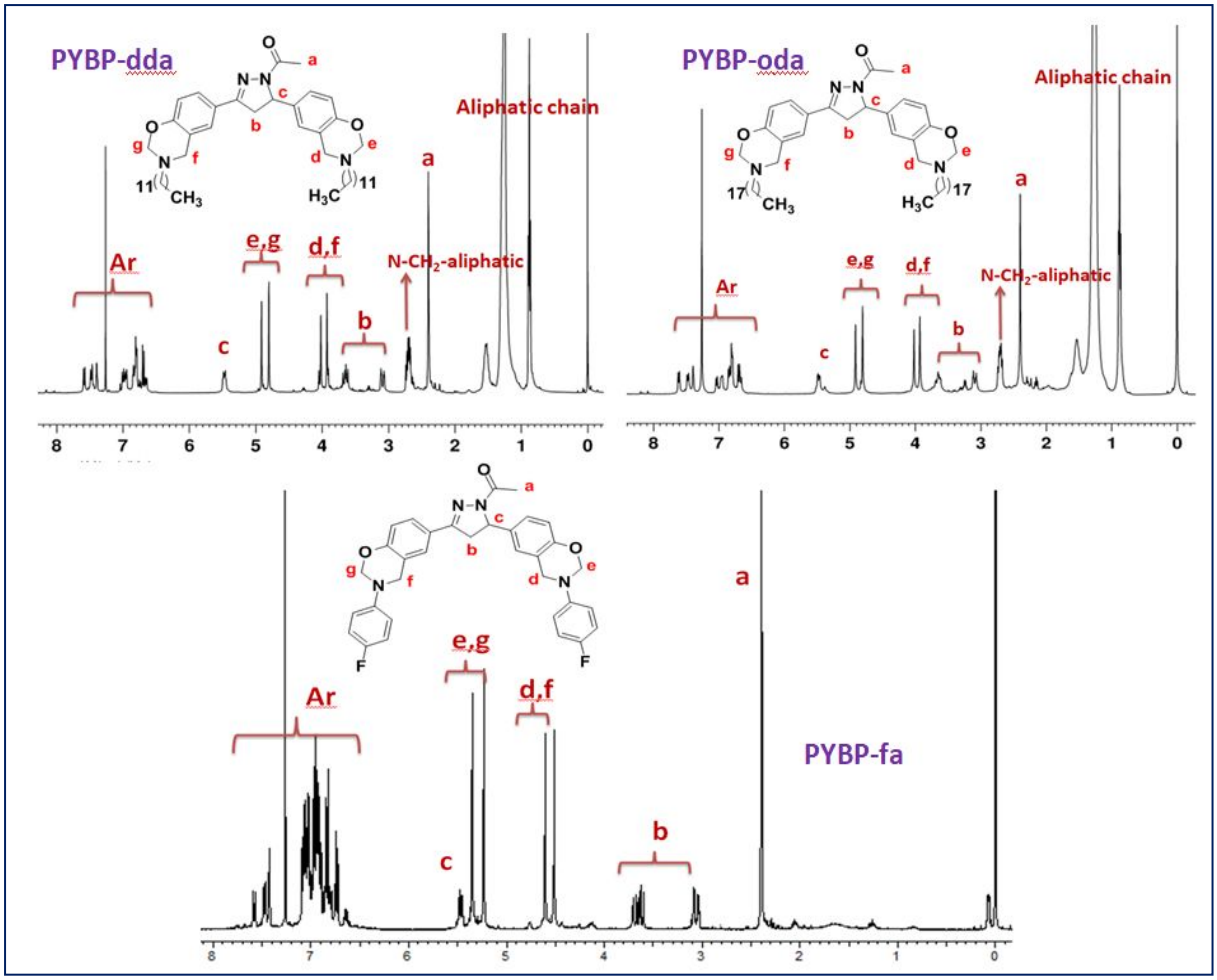

Figure 4. ^{1}H-NMR of monomers; PYBP-dda, PYBP-oda, PYBP-fa.

In case of BF-fa, the formation of benzoxazine ring was confirmed by two singlets at δ 4.5 and δ 5.2 ppm in its 1H-NMR spectrum. The methylene protons of BPF moiety appeared at δ 3.6 ppm. The ^{13}C-NMR spectrum of BF-fa (Figure S8) showed two signals at δ 65 and δ 79 ppm corresponding for the benzoxazine ring methylene carbons. The methylene carbon of the BPF moiety appeared at δ 60 ppm. The aromatic region shows excess peaks due to the interference of spin coupling of the fluorine atom. The quaternary carbon of the benzoxazine ring adjacent to oxygen atom appeared in the deshielding region at δ 152 ppm. The quaternary carbon attached to the fluorine atom appeared at δ 156 and δ 159 ppm.

The molecular structure of PYBP monomers was confirmed by ^{1}H-NMR and ^{13}C-NMR. Figure 4 represents the ^{1}H-NMR spectra of the monomers, PYBP-dda, PYBP-oda and PYBP-fa. In case of PYBP-dda, the formation of benzoxazine ring was confirmed by two sets of singlets at δ 3.8, δ 4.0 and δ 4.7, δ 4.9 ppm in its ^{1}H-NMR spectrum. The *N*-acetyl protons of PYBP moiety appeared at δ 2.4 ppm. Three sets of pyrazolidine ring protons are appeared

at δ 3.2, δ 3.7 and δ 5.4 ppm. The aliphatic chain protons are appeared at δ 0.8-1.8 ppm. The *N*-CH_2- protons showed a multiplet at δ 2.7 ppm. The ^{13}C-NMR spectrum of PYBP-dda (Figure S9) showed a signal at 20 ppm for *N*-acetyl group. The two sets of signals at δ 59 and δ 83 ppm correspond to the benzoxazine ring methylene carbons. The carbonyl carbon of the *N*-acetyl group appeared in the deshielding region at δ 168 ppm.

In case of PYBP-oda, the formation of benzoxazine ring was confirmed by two sets of singlets at δ 3.8, δ 4.0 and δ 4.7, δ 4.8 ppm in its 1H-NMR spectrum. The aliphatic chain appeared at δ 0.8-1.8 ppm. The *N*-acetyl protons of PYBP moiety appeared at δ 2.4 ppm. The *N*-CH_2- protons showed a multiplet at δ 2.7 ppm. Three sets of pyrazolidine ring protons are appeared at δ 3.2, δ 3.7 and δ 5.4 ppm. The ^{13}C-NMR spectrum of PYBP-oda (Figure S10) showed two signals at δ 59 and δ 83 ppm correspond to the benzoxazine ring methylene carbons. The carbonyl carbon of the *N*-acetyl group appeared in the deshielding region at δ 168 ppm. Mass spectrum of PYBP-oda is shown in Figure S11.

In case of PYBP-fa, the formation of benzoxazine ring was confirmed by two sets of singlets at δ 4.5, δ 4.6 and δ 5.2, δ 5.4 ppm in its 1H-NMR spectrum. The *N*-acetyl protons of PYBP moiety are appeared at δ 2.4 ppm. Three sets of pyrazolidine ring protons are appeared at δ 3.2, δ 3.7 and δ 5.4 ppm. The group of multiplets between 6.6 and 7.8 are attributed for aromatic protons. The ^{13}C-NMR spectrum of PYBP-fa (Figure S12) showed two signals at δ 59 and δ 83 ppm correspond to the benzoxazine ring methylene carbons. The aromatic region shows excess peaks due to the interference of spin coupling of the fluorine atom. The quaternary carbon attached to the fluorine atom appeared at δ 156 and δ 159 ppm. The carbonyl carbon of the *N*-acetyl group appeared in the deshielding region at δ 168 ppm.

3.3. Curing behaviour of benzoxazines

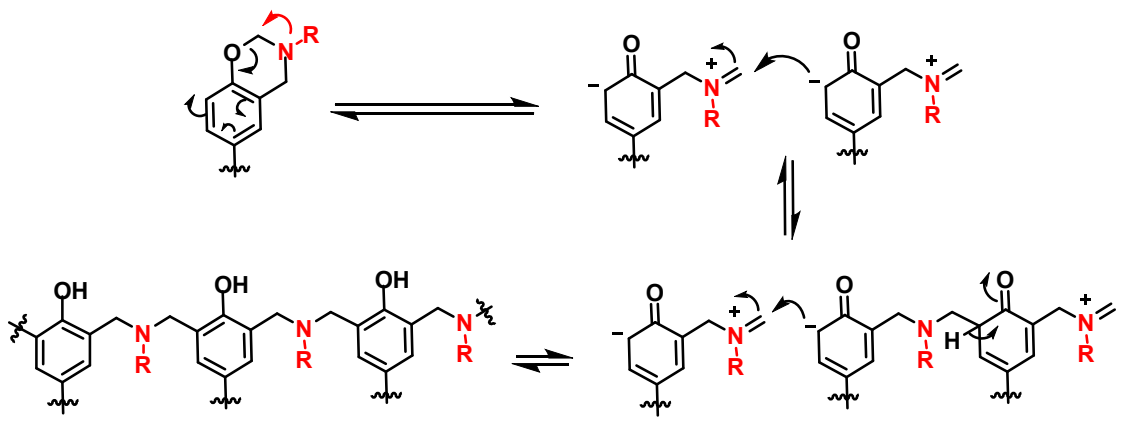

Scheme 3. General curing mechanism of benzoxazine monomer.

The ring opening polymerization of the prepared monomers is presented in Scheme 3. The lone pair on the nitrogen atom of the benzoxazine ring on heating drives the ring opening to create iminium nitrogen cation and a secondary carbanion. Further the secondary carbanion on this unstable structure reacts with the iminium cation followed by keto-enol tautomerism results in polymer network. The thermograms of BPF and PYBP monomers obtained from DSC are presented in Figures 5 and 6, respectively. The data on curing temperature of the above monomers are presented in Table 1.

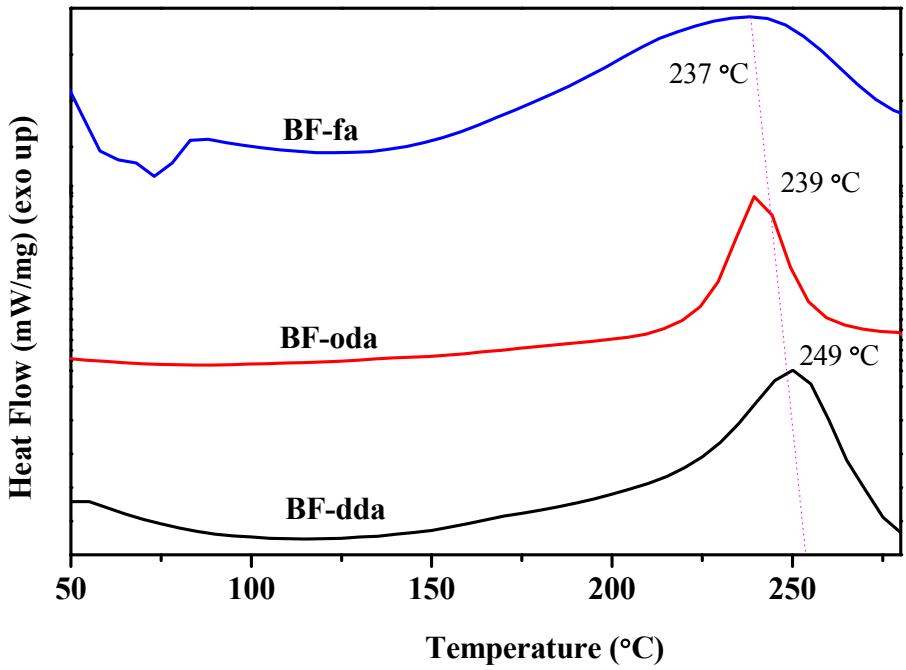

Figure 5. DSC curing curve of BPF based monomers.

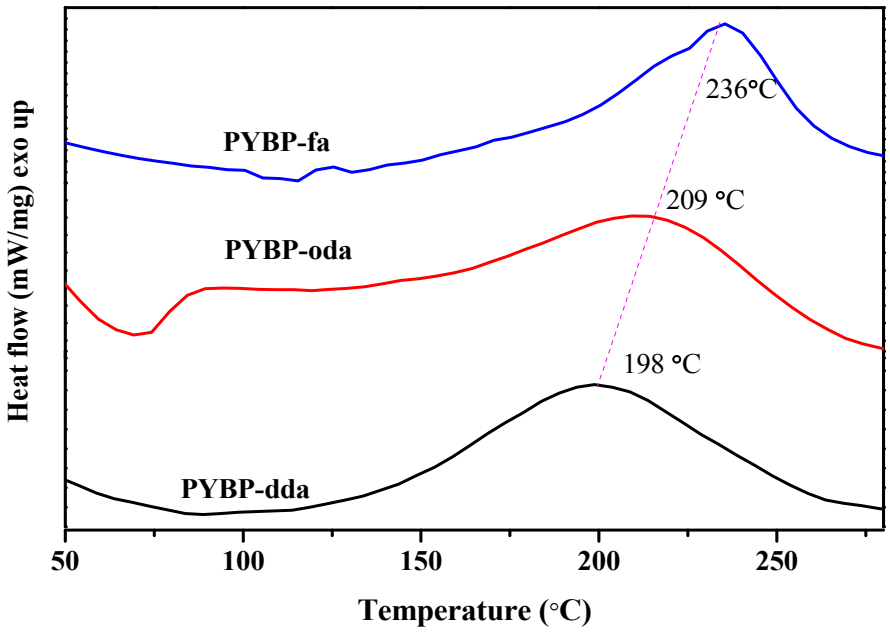

Figure 6. DSC curing curve of PYBP based monomers.

Table 1. Curing behaviours of BPF and PYBP monomers

Monomers	T_i (°C)	T_p (°C)	T_{final} (°C)	ΔH (mJ/mg)
BPF-dda	183	249	273	34
BPF-oda	209	239	275	35
BPF-fa	174	237	275	53
PYBP-dda	140	198	256	6
PYBP-oda	166	209	263	9
PYBP-fa	181	236	262	17

The curing onset of the BF-dda monomer starts at 183 °C and ends at 273 °C with the Tp at 249 °C. However, the curing onset of the PYBP-dda monomer starts at 140 °C and ends at 256 °C with Tp at 198 °C showing a decrease in the value of Tp of 50 °C when compared to that of BF-dda. Similarly, the curing of BF-oda starts at 209 °C and ends at 275 °C with Tp of 239 °C. The curing of PYBP-oda starts at 166 °C and ends at 263 °C with Tp of 209 °C and again show a decrease of 30 °C in the value of Tp when compared to that BF-oda. However, it was noticed that the fluoroaniline based benzoxazines, BF-fa and PYBP-fa have similar pattern of curing with Tp of 237 °C and 236 °C, respectively. Overall the curing temperatures of PYBP based benzoxazines are comparatively lower than that of BPF based

benzoxazines. This might be probably due to the presence of pyrazolidine ring which lowers the curing temperature. In addition, the PYBP based benzoxazine monomer liberates comparatively lower enthalpy than those of BF based monomers.

In the FTIR spectra (Figure 7) the disappearance of the peak appeared at 916 cm^{-1} represents the occurrence of ring opening polymerization reaction. Further, the peak at 1463 cm^{-1} corresponds to the trisubstituted benzene ring of the polymer. The peaks observed at 2948 cm^{-1} and 2893 cm^{-1} correspond to the asymmetric and symmetric stretching vibrations of methylene group (-CH_2-) of oxazine ring, respectively as well as long alkyl side chain of the dda and oda groups. The absence of peaks at 1242 cm^{-1} and 1090 cm^{-1} for the C-O-C bond of the benzoxazine monomer and the absence of peak at 1152 cm^{-1} for the asymmetric stretching of C-N-C of benzoxazine monomer clearly infer the occurrence of curing reactions.

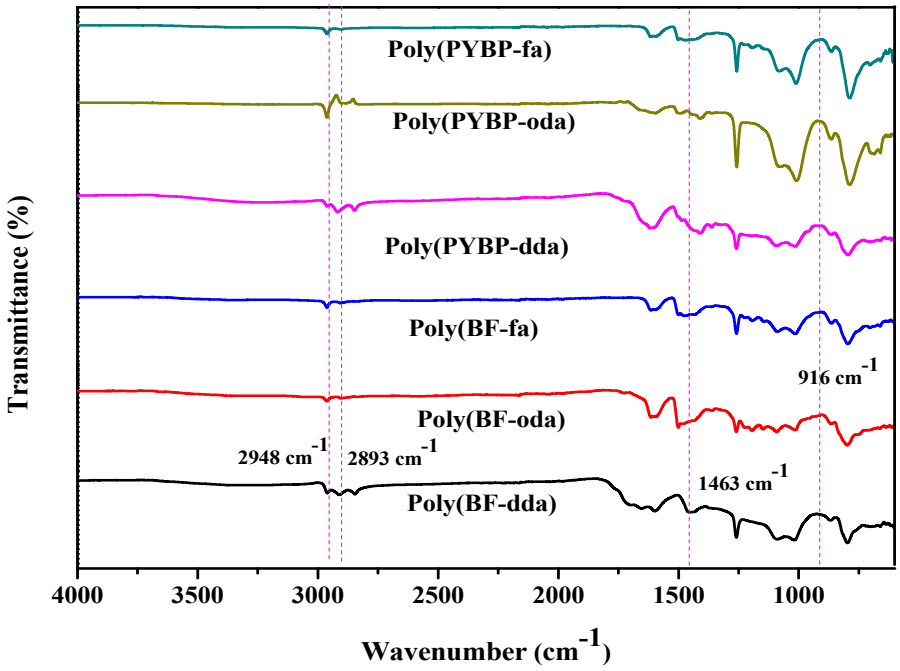

Figure 7. FTIR spectra of BPF and PYBP base Polybenzoxazines

3.4. Thermal Behaviour

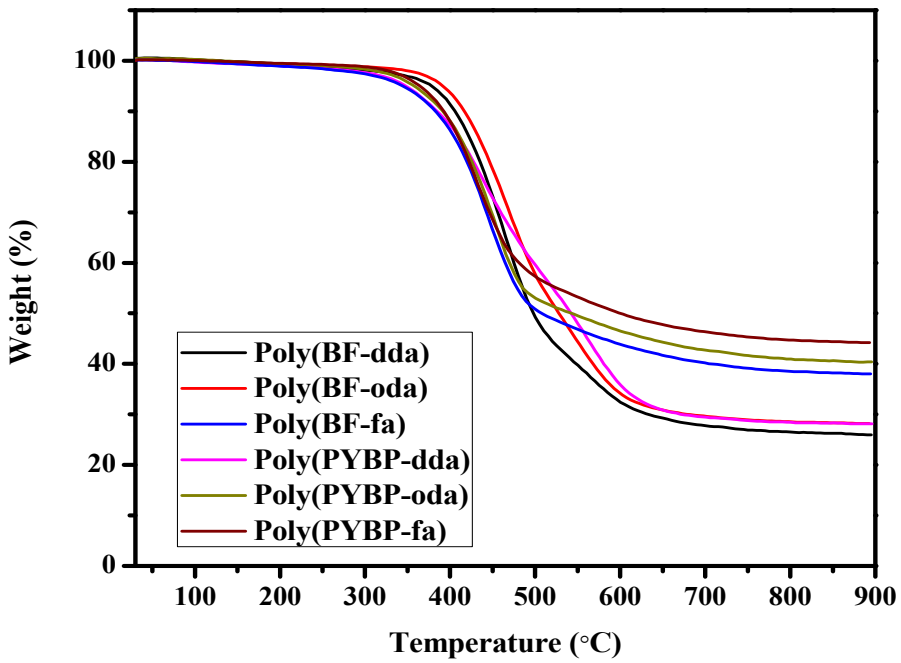

Figure 8. TGA of BPF and PYBP based Polybenzoxazines.

Table 2. Thermal behaviours of polymers

Sample	Degradation temperature (°C)			Char Yield % at 900 °C	LOI
	$T_{-5\%}$	$T_{-10\%}$	T_{max}		
Poly(BF-dda)	378	406	449	26	27.9
Poly(BF-oda)	391	414	461	29	29.1
Poly(BF-fa)	396	415	471	38	32.7
Poly(PYBP-dda)	340	373	422	28	28.7
Poly(PYBP-oda)	362	391	471	40	33.5
Poly(PYBP-fa)	365	395	510	44	35.1

The thermal stability of polymeric materials enhances their industrial utility mainly for high temperature and flame retardant applications. Hence, it is highly desirable to assess the thermal behaviour of benzoxazines prepared in the present work. The thermal stability was studied using TGA and the data obtained are presented in Figure 8 and Table 2.

The thermal degradation temperatures corresponding to 5 % and 10 % weight loss are presented in Table 2 along with its char yield obtained at 900 °C. The poly(BF-dda), poly(BF-oda) and poly(BF-fa) showed 5 % weight loss at 378 °C, 391 °C and 396 °C, respectively, and the poly(PYBP-dda), poly(PYBP-oda) and poly(PYBP-fa) showed 5 %

weight loss at 340 °C, 362 °C and 365 °C, respectively. The results were in quite similar pattern for 10 % weight loss. However, the maximum degradation temperature for poly(BF-dda), poly(BF-oda) and poly(BF-fa) are 449 °C, 461 °C and 471 °C which are quite similar to that of poly(PYBP-dda), poly(PYBP-oda) and poly(PYBP-fa) having maximum degradation temperature of 422 °C, 471 °C and 510 °C, respectively. Eventhough the 5 % and 10 % weight loss temperature for BPF based benzoxazine matrices were higher when compared to that of PYBP based benzoxazine matrices, the Tmax temperature of both the benoxazines were quite similar and higher than 400 °C. On the other hand the char yields of poly(BF-dda), poly(BF-oda) and poly(BF-fa) at 900°C were 26 %, 29 %, 38 %, respectively whereas the char yields of poly(PYBP-dda), poly(PYBP-oda) and poly(PYBP-fa) were 28 %, 40 %, 44 %, respectively. It is significant to mention that the char yields of the PYBP based benzoxazines were higher than that of the BPF based benzoxazines and this value directly influence and contributes to enhanced values of LOI. The LOI values were calculated using Van Krevelen and Hoftyzer relation between the char yield and LOI, which is given in equation 2.[37]

$$\mathrm{LOI} = 17.5 + 0.4(\mathrm{CR}) \quad \text{---------- (2)}$$

Here, CR is the percentage char yield of the sample remaining at 850 °C. It is experimentally proven that the materials having higher LOI values are flame retardant in nature.[38] The LOI of poly(BF-dda), poly(BF-oda) and poly(BF-fa) were 27.9, 29.1, 32.7, respectively whereas the LOI of poly(PYBP-dda), poly(PYBP-oda) and poly(PYBP-fa) are 28.7, 33.5, 35.1, respectively. In case of the pyrazolidine based benzoxazines, the poly(PYBP-oda) and poly(PYBP-fa) possesses the highest char yield and LOI values, which might be due to presence of thermally stable pyrazolidine heterocyclic core and fluorine atom of the aromatic side chain.

3.5 Morphological properties

In order to ascertain the micro structure of both BPF and PYBP based benzoxazines, the scanning electron microscopic (SEM) images were taken and are presented in Figure 9. Interestingly, the poly(BF-dda), poly(BF-oda) as well as poly(PYBP-dda), poly(PYBP-oda) showed roughness on its surface when compared to that of poly(BF-fa) and poly(PYBP-fa). In particular, the poly(BF-oda) and poly(PYBP-oda) showed wrinkled ripples morphology. The long chain octadecylamine present in both the cases showed jagged protrusion (Figures 9b and 9e). These rough surfaces can thus repel the water causing hydrophobicity. In case of

4-fluoroaniline monomers, poly(BF-fa) and poly(PYBP-fa) showed only smooth surfaces as attributed from the Figures 9c and 9f, respectively.

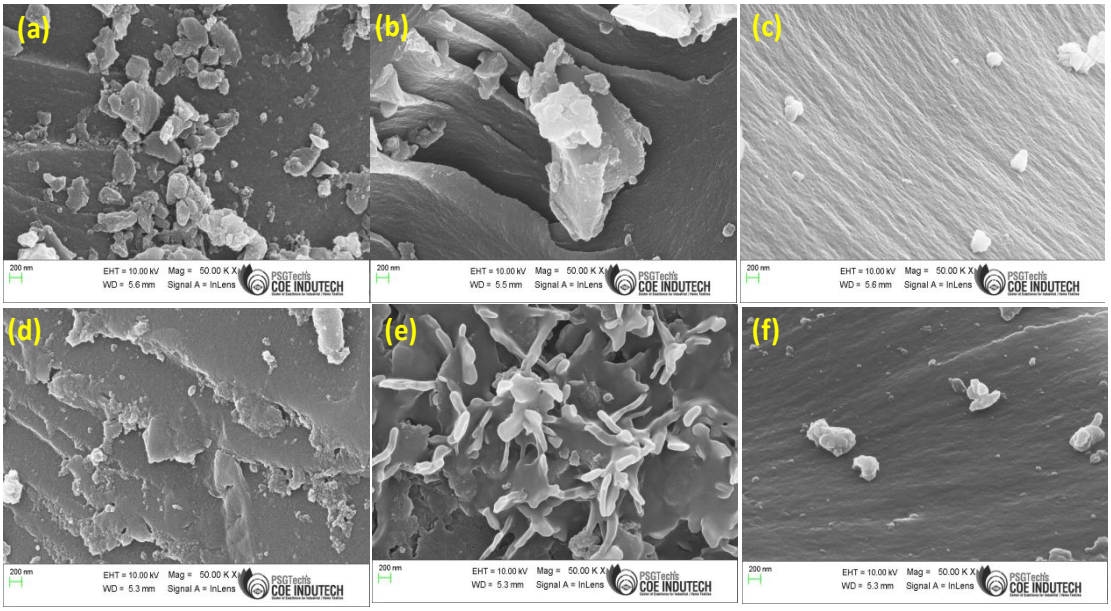

Figure 9. SEM images of (a) poly(BF-dd) (b) poly(BF-oda) (c) poly(BF-fa) (d) poly(PYBP-dda) (e) poly(PYBP-oda) (f) poly(PYBP-fa).

3.6. Curing analysis of the coated fabrics

Figures 10 and 11 represent the FTIR spectrum of the BPF based benzoxazines and PYBP based benzoxazines, respectively coated on the cotton fabrics. In the FTIR spectrum the treated fabrics showed peaks at 1705 cm^{-1} for carboxylic acid functional group and the peak appeared at 1246 cm^{-1} corresponds to C-O-C linkage. Since the fabric was treated with sodium hydroxide, the secondary hydroxyl group might be oxidised to the carboxylic group. After coating with the polymer, the fabric was cured at two different temperatures, one at 180 °C and other at 250 °C.

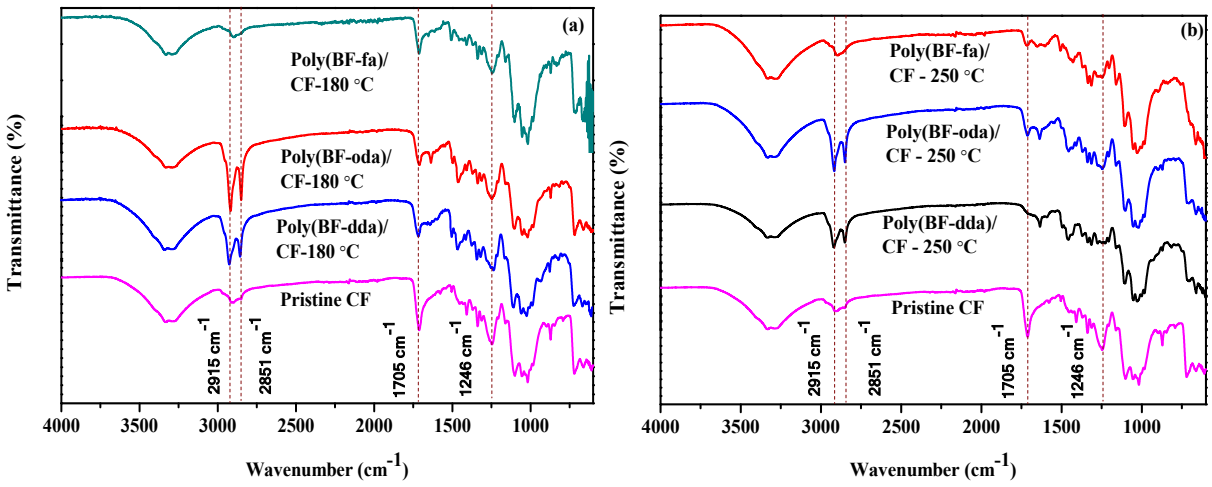

Figure 10. FTIR Spectra of pristine fabric and BPF based benzoxazine coated cotton fabrics (CF).

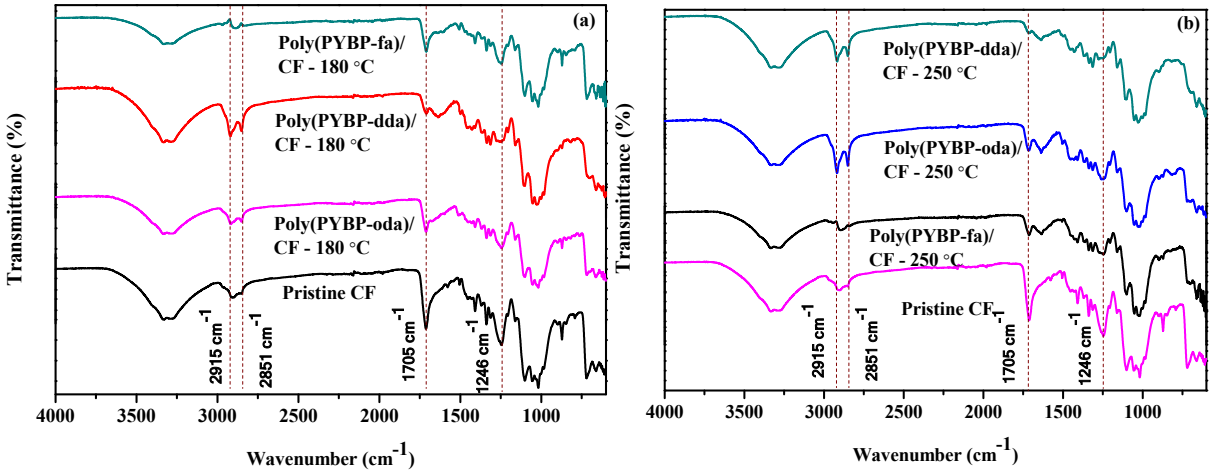

Figure 11. FTIR Spectra of pristine fabric and PYBP based benzoxazine coated fabrics (CF).

The FTIR spectra of the pristine fabric are compared with fabrics coated with BPF based benzoxazine (Figures 10a-b) or PYBP based benzoxazine (Figures 11a-b). From the Figures 10 and 11, it is clear that the peaks appeared at 1705 cm^{-1} and 1246 cm^{-1} are still present when the curing temperature is 180 °C (Figures 10a and 11a) whereas those peaks are completely disappeared when the curing temperature is raised to 250 °C (Figures 10b and 11b). This infers that at 250 °C complete curing process takes place and the benzoxazine polymers binds chemically with the functional groups present in the cotton fabrics.

3.7. XPS analysis

In order to ascertain the interaction between benzoxazine and cotton, the poly(PYBP-oda) coated cotton fabric was subjected to XPS analysis and presented in Figure 12 in comparison with that of pristine fabric. The pristine fabric shows the presence of carbon and oxygen alone at 283 and 531 eV, respectively. However, the poly(PYBP-oda) coated cotton shows the presence of nitrogen in addition to carbon and oxygen at 399 eV. This presence of N atom confirms that the coating of polybenzoxazines on the cotton surface has been achieved successfully through the thermal ring opening polymerization of oxazine moiety. Also, the elemental profiles are found to be varied significantly. The pristine cotton possess 26.9 % of oxygen and 73 .1 % of carbon. The poly(PYBP-oda) coated cotton exhibits 5.5 % of oxygen, 89.8 % of carbon and 4.7 % of nitrogen. The decrease in the percentage of oxygen, increase in the percentage of carbon and presence of smaller quantity of nitrogen strongly suggest that the coating of polybenzoxazine has been achieved successfully.

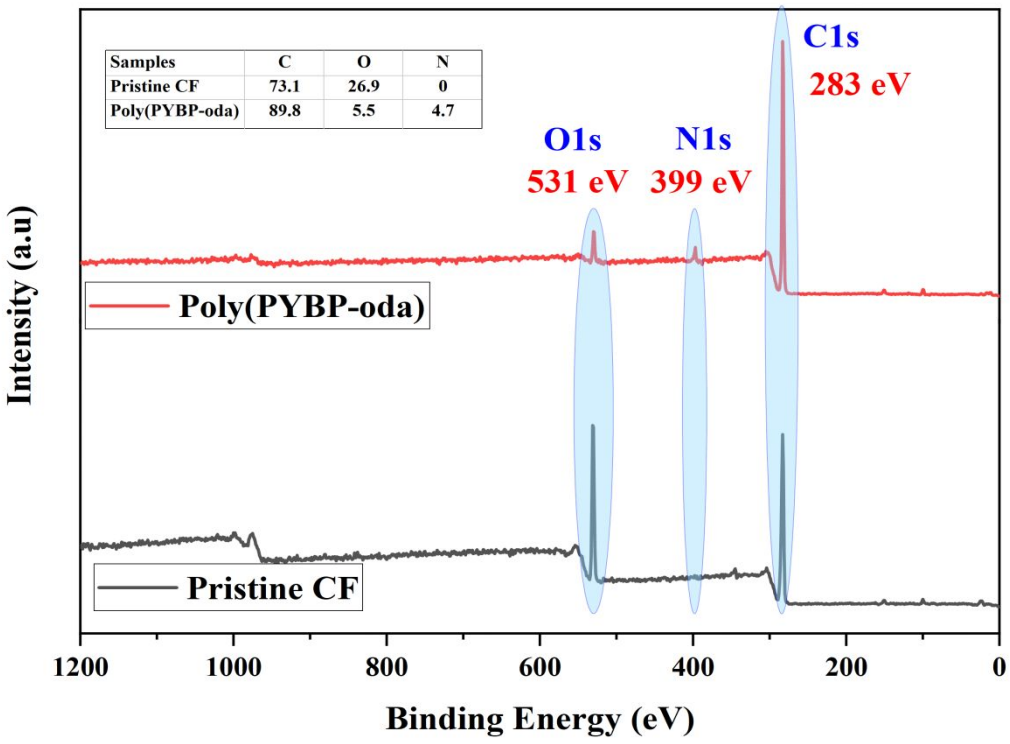

Figure 12. XPS analysis of PYBP-oda coated cotton fabric and pristine cotton fabric

In addition, the binding nature was intensively ascertained from the deconvoluted binding energy curves of carbon atom of both pristine and poly(PYBP-oda) coated fabrics (Figure 13). The pristine atom delivers three significant peaks at 286.0, 284.1 and 282.4 eV, which are all attributed to the carbon atoms of C=O, C-O and C-C bonding environment, respectively. However, on the other hand, the poly(PYBP-oda) coated fabric shows a major

peak at 282.6 eV and a minor peak at 284.3 eV. This infers that the polar functional groups of the fabrics namely C-O, and C=O might undergone cross-linking during the thermal treatment aided for the curing of benzoxazines. Thus, the coating of poly(PYBP-oda) on cotton fabric favours more hydrophobic behaviour due to presence of non-polar and low surface energy polybenzoxazine layer.

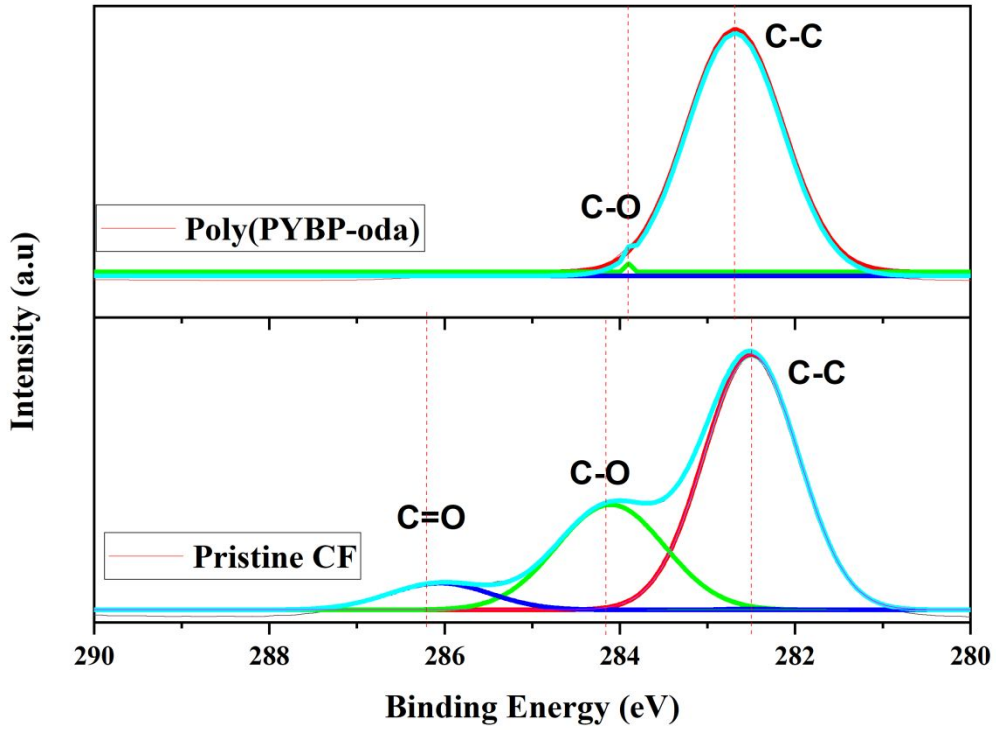

Figure 13. Deconvoluted binding energy curve of the carbon presented in PYBP-oda coated cotton fabric and pristine cotton fabric

3.8. Water Contact Angle (WCA)

The water contact angles (WCA) of the prepared polymers are presented in Figures 14-15. The pristine cotton fabric shows no contact angle value, which is due to the absorption of water droplet. However, the WCA of poly(BF-dda), poly(BF-oda) and poly(BF-fa) coated fabrics are 139.7°, 151.5° and 144.3°, respectively in Figure 14. The octadecyl long chain based poly(BF-oda) showed higher WCA, due to the oleophilic nature of the alkyl chain. Whereas, in case of poly(PYBP) based benzoxazines (Figure 15), the WCA of poly(PYBP-dda), poly(PYBP-oda) and poly(PYBP-fa) are 143.1°, 154.7° and 151.8°, respectively. Here also the octadecyl alkyl chain have influenced the WCA to 154.7° which is the highest value observed among the different benzoxazines prepared in the present work. In addition, the sliding contact angle value of poly(PYBP-oda) was also observed to be 9°, which is found to

be less than 10°. The sliding contact angle value observed for poly(PYBP-oda) is almost equivalent to that of bisphenol-A based polybenzoxazine coated fabric (9°) reported earlier[30]. The poly(PYBP-oda) prepared in the present work can be used as better coating material modify the surface of cotton fabrics with superhydrophobic characteristics.

Figure 14. Contact angle images of BPF based benzoxazines coated fabrics.

Figure 15. Contact angle images of PYBP based benzoxazines coated fabrics.

3.9. Morphology of polybenzoxazine coated cotton fabrics

The dodecyl alkyl chain showed the best WCA, *i.e*. poly(BF-oda) showed 151.5° and poly(PYBP-oda) showed 154.7°. Hence these two samples were analysed for SEM images. The SEM images of pristine cotton fabrics are shown in Figures 16a and 16b. Figure 16c and 16d are the representative SEM images of poly(BF-oda) and Figures 16e and 16f corresponds for the SEM images of poly(PYBP-oda). From the Figures 16a and 16b, it is clear that the pristine fabric has uniform surface layers. After coated with poly(BF-oda) as represented in Figures 16c and 16d or poly(PYBP-oda) as represented in Figures 16e and 16f, the surface of the cotton fabric has rough surfaces and protrusion which is the reason for the coated cotton fabric to exhibit higher WCA upto 154.7°.

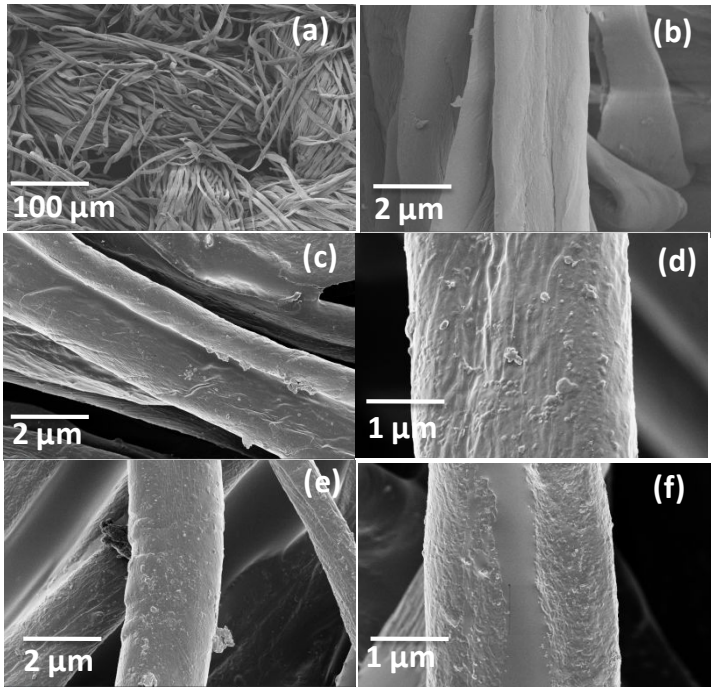

Figure 16. SEM images of (a-b) pristine fabric, (c-d) Poly(BPF-oda) and (e-f) Poly(BYPA-oda) coated cotton fabrics.

3.10. Oil-Water separation

Among the benzoxazine samples studied the poly(PYBP-oda) coated cotton fabric displayed the highest WCA 154.7° and preferred to be the most suitable sample for oil-water separation. Hence it was tested for the application in oil-water separation. Prior to that water and oil were dropped on the cotton fabric. It was interesting to see that the water forms a droplet whereas the oil was absorbed on the fabric (Figure 17a, Supporting information video).

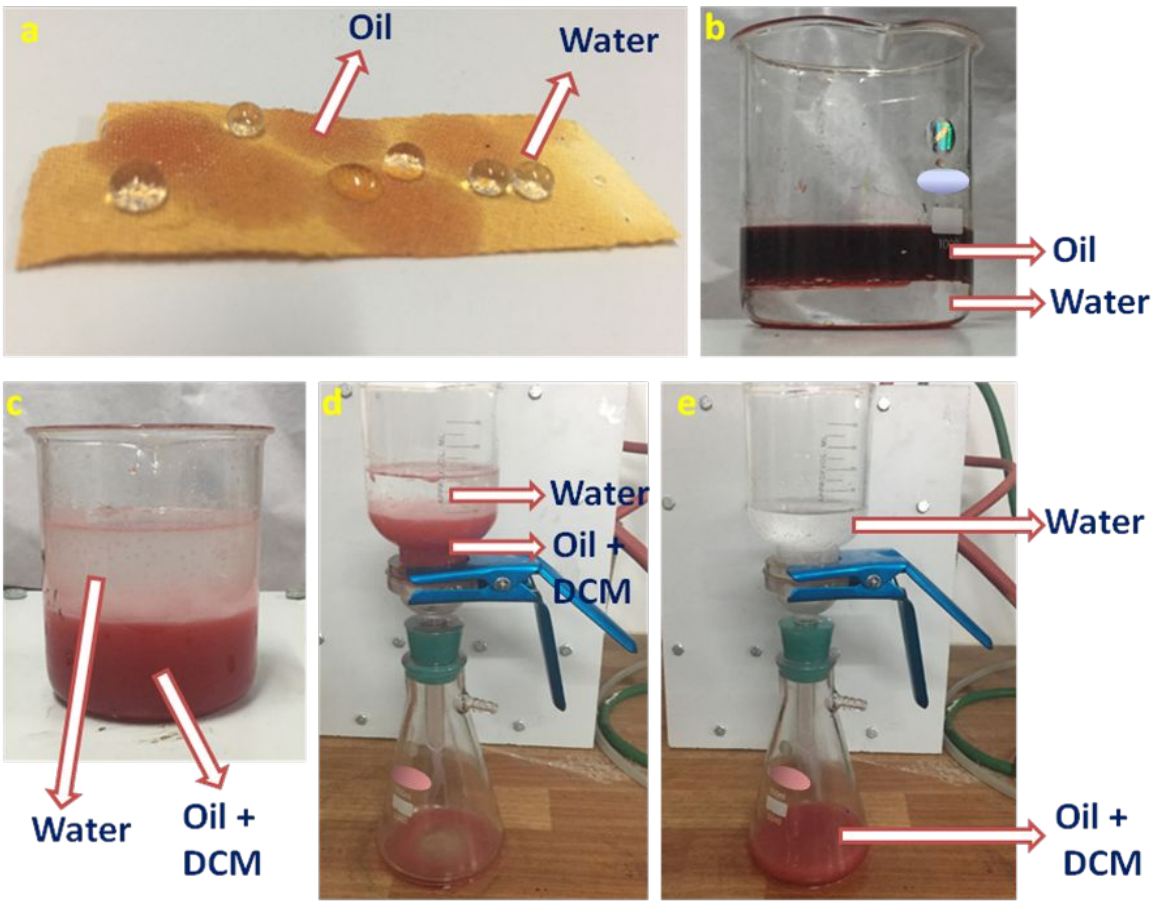

Figure 17. Separation process of oil and water a) Photograph of the water droplet and oil on poly(PYBP-oda) coated fabric, b) Oil and water taken in a beaker, c) Mixture of oil, water and dichloromethane (DCM), d) Mixture of oil, water and DCM in a separation flask, e) Separated position of oil dissolved in DCM and water

For the oil-water separation experiment, a mixture of water (100 mL) and engine oil (20W40 grade with density 0.88, 100 mL) were taken in a beaker, where the low density oil forms the top layer and water at the bottom (Figure 17b). Since the oil-water separation experiment cannot be done with this criteria, the oil layer was brought down to the bottom by the addition of dichloromethane (DCM) solvent (100 mL). Water (100 mL) was added again to make equal volume. Now just by stirring, the density of oil and DCM mixture gets denser and settled as bottom layer while the water takes up the top layer (Figure 17c). For the oil-water separation experiment, the poly(PYBP-oda) cotton fabric was fixed between a glass funnel and a conical flask with an effective separation area of 12.6 cm^2. The mixture of water, oil and DCM was added to the funnel of the separation flask (Figure 17d). The oil present in DCM layer permeated quickly through the poly(PYBP-oda) coated micro structured layer of cotton fabric and was collected in the filtration flask. However, water layer did not permeate due to repulsion and hydrophobic nature (Figure 17e). It was interesting to

note that the oil layer permeated through the cotton fabric only due to gravity and no external pressure was applied.

The commercial impact of the superhydrophobic materials for their application in the oil-water separation relies in the recycling performance. Hence, the oil-water experiment was repeated for 10 cycles and the recycling performance was observed. The recycling performance can be measured by the separation efficiency (Figure 18a) and the flux of the material (Figure 18b) after each cycle of the oil-water separation. The separation efficiency was calculated from the equation 3.

$$\text{Separation efficiency} = \frac{Volume\ of\ \text{the}\ oil\ before\ separation}{Volume\ of\ \text{the}\ oil\ after\ separation} X\ 100 \quad \ldots\ldots\ldots\ldots\ldots\ldots (3)$$

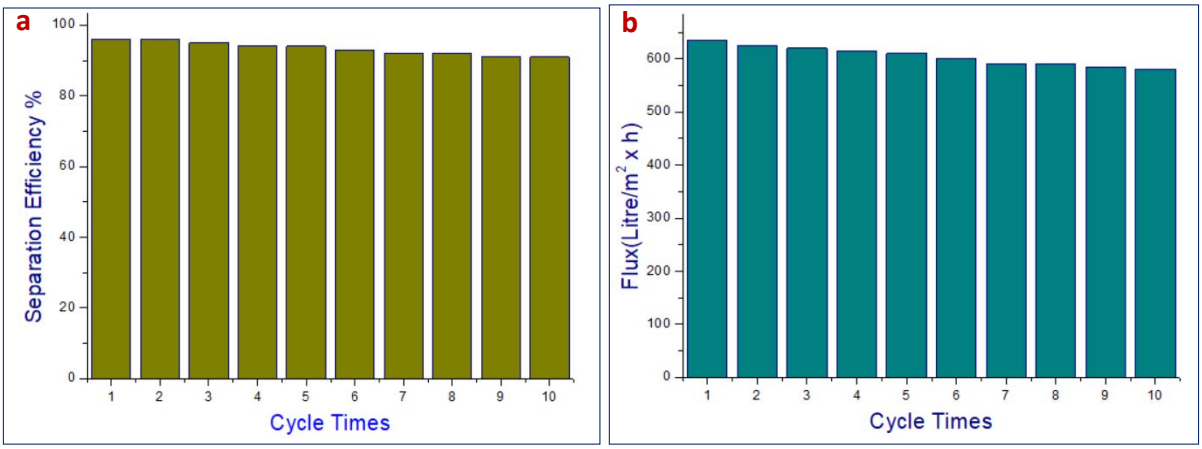

Figure 18. a) Separation efficiency (%) and b) flux (Litre/m^2 x h) of the poly(PYBP-oda) for oil-water separation.

The flux of a material during the oil-water separation was calculated from the equation 4.[38]

$$Flux = \frac{Volume\ of\ \text{the}\ permeated\ oil}{Area\ of\ \text{the}\ fabric\ X\ time\ for\ separation} \quad \ldots\ldots\ldots\ldots\ldots\ldots (4)$$

From the Figure 16a, the separation efficiency (%) of the poly(PYBP-oda) coated fabric can be noted for each cycles of oil-water separation. Initially the separation efficiency was 96 % and after 10 cycles the efficiency was 91 %. From this data it is clear that even after 10 cycles of oil-water separation efficiency of the poly(PYBP-oda) was > 90 % confirming its sustainable hydrophobic behaviour. Figure 16b show the impact of the poly(PYBP-oda) coated cotton material on the oil-water separation process as represented by flux of the material (litre/area in m^2 x time in h). For the first cycle the flux was 635 L/m^{2}h. After 10 cycles the flux of the poly(PYBP-oda) just reduced to 580 L/m^{2}h showing > 90 %

effectiveness. The separation efficiency observed for poly(PYBP-oda) coated fabric is almost equivalent to that of reported cotton fabrics coated with bisphenol-A based polybenzoxazine[30]. Thus, the synthesized pyrazolidine based benzoxazines provide an insight that the benzoxazine substituted with heterocycles can be an alternative for bisphenol derivative.

Table 3. Physical properties of cotton

Samples	Average Porosity (micron)	Tensile strength (MPa)
Pristine cotton fabric	28.2	13.3
Poly(PYBP-oda)/Cotton	25.7	28.5

Further, the investigations with respect to primary properties of the cotton fabrics were also carried out. Hence, pore size distribution (Figure S13a-b) and tensile strength of the pristine and PYBP-oda coated fabrics were analyzed and presented in Table 3. The average pore size distribution of pristine fabric is 28.2 micron (Figure S13a), whereas that of the poly(PYBP-oda) coated fabric is 25.7 micron (Figure S13b). This result suggests that even after coating the overall porosity of the fabric is not changed significantly. This infers that the surface coating has been achieved without altering the porous nature of pristine fabric. Further, the tensile strength of pristine fabric was also observed to increase from 13.3 Mpa to 28.5 MPa after coating with poly(PYBP-oda). This might be due to the enhancement of stiffness of the fibers caused by the coated polybenzoxazine.

4. CONCLUSION

The replacement of toxic bisphenol-A based benzoxazine with less toxic bisphenol-F (BF) based benzoxazine and non-toxic pyrazolidine (PYBP) based benzoxazine and their application towards the fabrication of superhydrophobic/superoleophilic cotton was achieved. In this respect, the synthesized benzoxazines hold hydrophobic part derived from amines with inherent hydrophobic behaviour such as dodecylamine (dda), octadecylamine (oda) and 4-fluoroaniline (fa). Among them, the octadecyl derivative, poly(BF-oda) as well as poly(PYBP-oda) showed an excellent WCA values higher than 150°. In particular, poly(PYBP-oda) exhibited the highest WCA = 154.7°. The rough surfaces observed in the SEM images of the poly(PYBP-oda) coated fabrics also supported its hydrophobic nature. Finally, the poly(PYBP-oda) coated fabric was analysed for oil-water separation. The separation efficiency was found to be greater than 90 % after 10 cycles and flux was just reduced from 635 L/m^{2}h to 580 L/m^{2}h. The greater separation efficiency and the flux of the

poly(PYBP-oda) indicate that the newly developed polybenzoxazine discussed in the present study can be used as effective hydrophobic/oleophilic material when coated on cotton fabric for oil-water separation applications.

Acknowledgment

The authors thank the PSG Management for their moral and financial support. Also, the authors acknowledge the SIF, VIT, Vellore for providing NMR facility and CLIF, University of Kerala for providing XPS facility.

Conflict of Interest

The authors have no conflict of interest.

***Supporting Information**

The Supporting Information is available free of charge on the ACS Publications website.

Experiment part describing evaluation of cytotoxicity, Table S1 and Figure S1-S13

References

(1) Takeichi, T.; Kawauchi, T.; Agag, T. High performance polybenzoxazines as a novel type of phenolic resin. *Polym. J*. **2008**, *40*, 1121.

(2) Ishida, H.; Krus, C.M. Synthesis and characterization of structurally uniform model oligomers of polybenzoxazine. *Macromolecules*. **1998**, *31*, 2409.

(3) Gnanapragasam, S.; Krishnan, S.; Arumugam, H.; Chavali, M.; Alagar, M. Synthesis and characterization of a novel high-performance benzoxazine from benzaldehyde-based bisphenol. *Adv. Polym. Tech*. **2018**, *37*, 3056.

(4) Kiskan, B.; Ghosh, N.N.; Yagci, Y. Polybenzoxazine-based composites as high-performance materials. *Polym. Int*. **2011**, *60*, 167.

(5) Ishida, H.; Agag, T. Handbook of benzoxazine resins. Elsevier: **2011**.

(6) Okada, H.; Tokunaga, T.; Liu, X.; Takayanagi, S.; Matsushima, A.; Shimohigashi, Y. Direct evidence revealing structural elements essential for the high binding ability of bisphenol A to human estrogen-related receptor-γ. *Environ. Health Perspec*. **2007**,*116*, 32.

(7) Lehmler, H.J.; Liu, B.; Gadogbe, M.; Bao, W. Exposure to bisphenol A, bisphenol F, and bisphenol S in US adults and children: The national health and nutrition examination survey 2013–2014. *ACS omega*. **2018**, *3*, 6523.

(8) Baluka, S.A.; Rumbeiha, W.K. Bisphenol A and food safety: Lessons from developed to developing countries. *Food Chem. Toxicol*. **2016**, *92*, 58.

(9) Liu, Y.; Yue, Z.; Gao, J. Synthesis, characterization, and thermally activated polymerization behavior of bisphenol-S/aniline based benzoxazine. *Polymer*. **2010**, *51*, 3722.

(10) Liu, J.; Ishida, H. Anomalous isomeric effect on the properties of bisphenol f-based benzoxazines: Toward the molecular design for higher performance. *Macromolecules*. **2014**, *47*, 5682.

(11) European Chemicals Agency, Analysis of SIN LIST. (for bisphenol-F) https://echa.europa.eu/documents/10162/19126370/sinlist_analysis_en.pdf/6248cac0-ffa8-5a14-ae55-93ace7ee9017.

(12) https://echa.europa.eu/documents/10162/769b2777-19cd-9fff-33c4-54fe6d8290d5

(13) Rochester, J.R.; Bolden, A.L. Bisphenol S and F: a systematic review and comparison of the hormonal activity of bisphenol A substitutes. *Environ. Health perspect.* **2015**, *123*, 643.

(14) Salum, M.L.; Iguchi, D.; Arza, C.R.; Han, L.; Ishida, H.; Froimowicz, P. Making Benzoxazines Greener: Design, Synthesis, and Polymerization of a Biobased Benzoxazine Fulfilling Two Principles of Green Chemistry. *ACS Sustain. Chem. Eng.* **2018**, *6*, 13096.

(15) Ergin, M.; Kiskan, B.; Gacal, B.; Yagci, Y. Thermally curable polystyrene via click chemistry. *Macromolecules*. **2007**, *40*, 4724.

(16) Kiskan, B.; Demiray, G.; Yagci, Y. Thermally curable polyvinylchloride via click chemistry. *J. Polym. Sci. Pol. Chem*. **2008**, *46*, 3512.

(17) Kukut, M.; Kiskan, B.; Yagci, Y. Self-curable benzoxazine functional polybutadienes synthesized by click chemistry. *Des. Monomers Polym*. **2009**, *12*, 167.

(18) Nagai, A.; Kamei, Y.; Wang, X.S.; Omura, M.; Sudo, A.; Nishida, H.; Kawamoto, E.; Endo, T. Synthesis and crosslinking behavior of a novel linear polymer bearing 1, 2, 3-triazol and benzoxazine groups in the main chain by a step-growth click-coupling reaction. *J. Polym. Sci. Pol. Chem*. **2008**, *46*, 2316.

(19) Hariharan, A.; Srinivasan, K.; Murthy, C.; Alagar, M. A novel imidazole-core-based benzoxazine and its blends for high-performance applications. *Ind. Eng. Chem. Res.* **2017**, *56*, 9347.

(20) Hariharan, A.; Kesava, M.; Alagar, M.; Dinakaran, K.; Subramanian, K. Optical, electrochemical, and thermal behavior of polybenzoxazine copolymers incorporated with tetraphenylimidazole and diphenylquinoline. Polym. Adv. Tech. **2018**, *29*, 355.

(21) Selvi, M.; Devaraju, S.; Vengatesan, M.R; Alagar, M. Synthesis and characterization of heterocyclic core-based polybenzoxazine matrices. *J. Appl. Polym*. **2019**, *136*, 47134.

(22) Lee, H.J.; Owens, J. Superhydrophobic Superoleophobic Woven Fabrics. In *Advances in Modern Woven Fabrics Technology* Vassiliadis, S, Ed, **2011**. IntechOpen.

(23) Ma, M.; Hill, R.M. Superhydrophobic surfaces. Curr. Opin. Colloid Interface Sci. **2006**, *11*, 193.

(24) Zhang, X.; Shi, F.; Niu, J.; Jiang, Y.; Wang, Z. Superhydrophobic surfaces: from structural control to functional application. J. Mater. Chem. **2008**, *18*, 621.

(25) Tuteja, A.; Choi, W.; Mabry, J.M.; McKinley, G.H.; Cohen, R.E. Robust omniphobic surfaces. *Proc. Natl. Acad. Sci*. **2008**, *105*, 18200.

(26) Liu, K.; Tian, Y.; Jiang, L. Bio-inspired superoleophobic and smart materials: design, fabrication, and application. *Prog. Mater. Sci.* **2013**, *58*, 503.

(27) Nishimoto, S.; Bhushan, B. Bioinspired self-cleaning surfaces with superhydrophobicity, superoleophobicity, and superhydrophilicity. *RSC Adv.* **2013**, 3, 671.

(28) Zhang, W.; Lu, X.; Xin, Z.; Zhou, C. A self-cleaning polybenzoxazine/TiO_2 surface with superhydrophobicity and superoleophilicity for oil/water separation. *Nanoscale.* **2015**, *7*, 19476.

(29) Liu, C.T.; Su, P.K.; Hu, C.C.; Lai, J.Y.; Liu, Y.L. Surface modification of porous substrates for oil/water separation using crosslinkable polybenzoxazine as an agent. *J. Membrane Sci.* **2018**, *546*, 100.

(30) Li, Y.; Yu, Q.; Yin, X.; Xu, J.; Cai, Y.; Han, L.; Huang, H.; Zhou, Y.; Tan, Y.; Wang, L.; Wang, H. Fabrication of superhydrophobic and superoleophilic polybenzoxazine-based cotton fabric for oil–water separation. *Cellulose*. **2018**, 25, 6691.

(31) Lin, Z.; Liu, Y.; Wong, C.P. Facile fabrication of superhydrophobic octadecylamine-functionalized graphite oxide film. *Langmuir.* **2010**, *26*, 16110.

(32) Zhou, Z; Zhuo, J; Yan, S; Ma, L. Design and synthesis of 3, 5-diaryl-4, 5-dihydro-1*H*-pyrazoles as new tyrosinase inhibitors. *Bioorg. Med. Chem.* **2013**, *21*, 2156.

(33) Vimala, K.; Sundarraj, S.; Paulpandi, M.; Vengatesan, S.; Kannan, S. Green synthesized doxorubicin loaded zinc oxide nanoparticles regulates the Bax and Bcl-2 expression in breast and colon carcinoma. *Process Biochem*. **2014**, *49*, 160.

(34) Thennarasu, P.; Prabunathan, P.; Senthilkumar, M. Development of biomass-derived functionalized activated carbon-coated and polyaniline-grafted cotton fabric with enhanced ultraviolet resistance. *J. Ind. Text.* **2018**, *47*, 1609.

(35) Ning, X.; Ishida, H. Phenolic materials via ring-opening polymerization: Synthesis and characterization of bisphenol-A based benzoxazines and their polymers. *J. Polym. Sci. Pol. Chem.* **1994**, *32*, 1121.

(36) Allen, D.J.; Ishida, H. Polymerization of linear aliphatic diamine-based benzoxazine resins under inert and oxidative environments. *Polymer*. **2007**, *48*, 6763.

(37) Van Krevelen, D.W.; Hoftyzer, P.J. Properties of Polymers, 2nd ed. Elsevier, New York, 1976.

(38) Gao, J.; Huang, X.; Xue, H.; Tang, L.; Li, R.K. Facile preparation of hybrid microspheres for super-hydrophobic coating and oil-water separation. *Chem. Eng. J.* **2017**, *326*, 443.

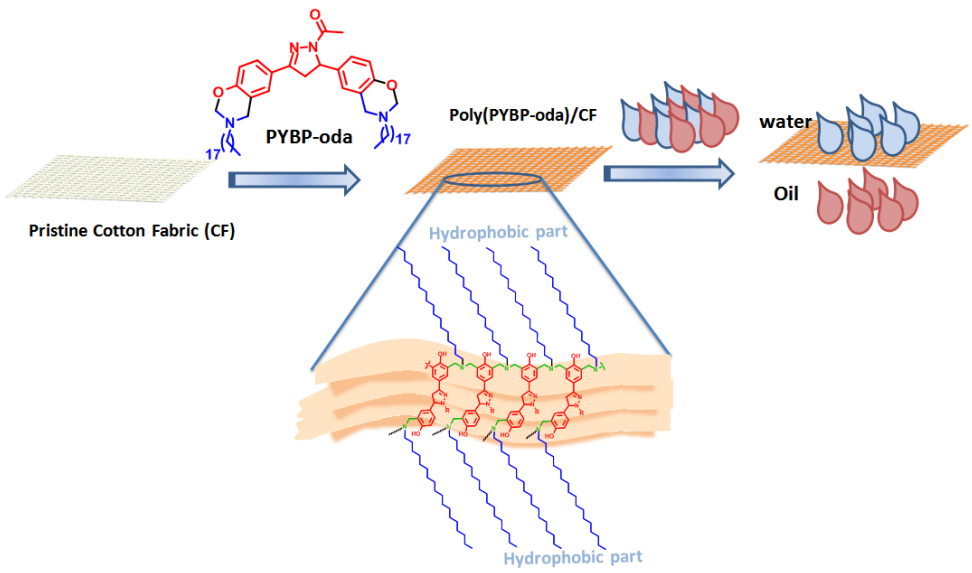

Graphical Abstract

292x167mm (96 x 96 DPI)